Trees
DOI 10.1007/s00468-013-0867-z

ORIGINAL PAPER

The effect of crown architecture on dynamic amplification factor of an open-grown sugar maple (*Acer saccharum* L.)

Cihan Ciftci · Sergio F. Brena · Brian Kane · Sanjay R. Arwade

Received: 2 October 2012 / Revised: 18 February 2013 / Accepted: 19 February 2013

Abstract Tree failure may cause significant economic and societal disruptions in urban environments. A better understanding of the relationship between branches and stem as they affect the dynamic response of decurrent trees under wind loading is needed to reduce the risk of tree failure. Finite element (FE) models were used to identify the parameters that primarily impact tree response. A base model was developed using data from a sugar maple (*Acer saccharum* L.) located in Belchertown, MA, USA, from which parametric models were subsequently developed. Confidence in the base model was gained by comparing the natural frequency of this tree with experimental results. Results from a parametric study incorporating changes in eight different tree parameters (stem diameter, slenderness ratio of branches, number of branches, damping ratio, branch attachment heights, branch attachment angles, branch azimuth angles, and elastic modulus) are then presented to help identify critical model properties that affect the dynamic amplification factor (Rd) of the tree. A single parameter was varied in each model while keeping others unchanged from the base model. Parameters with the greatest effect on Rd included stem diameter, number and slenderness of branches in the crown, elastic modulus of stem and branches, and damping ratio. Thus, it may be possible to use pruning to alter crown architecture to reduce the risk of tree failure.

Keywords Sway frequency · Oscillation · Dynamic analysis · Damping ratio · Maple · Wind

Introduction

In developed landscapes, trees provide many benefits (Nowak and Dwyer 2007), which accrue mostly from larger trees (Nowak et al. 2002). However, if they fail, large trees are more likely to cause property damage and personal injury. Wind is a primary cause of tree failure, and much work has been conducted to develop mechanistic models predicting critical wind speeds at which failure of forest trees will occur (see Gardiner et al. 2008 for a review). A large body of knowledge has investigated windthrow and trunk breakage under static loading (Peltola 2006), but very few studies have considered large, open-grown trees (Kane and Clouston 2008). It has also long been recognized that predictions of critical wind speeds from static winching tests are overestimates since they do not capture the dynamic interaction of wind and tree (Oliver and Mayhead 1974). The dynamic amplification factor, which is described below, is the ratio of dynamic to static displacements (Chopra 2007) and has previously been used to investigate the dynamic response of trees (Sellier and Fourcaud 2009).

Investigations of tree dynamics have been both empirical (Blackburn et al. 1988; Baker 1997; Moore and Maguire 2005; James et al. 2006; Spatz et al. 2007; Rodriguez et al. 2008; Kane and James 2011) and theoretical (Baker 1995; Kerzenmacher and Gardiner 1998; Saunderson et al. 1999; England et al. 2000). Finite element modeling has also been used to investigate the effect of crown architecture and

Communicated by T. Fourcaud.

C. Ciftci (✉) · S. F. Brena · S. R. Arwade
Department of Civil and Environmental Engineering, University of Massachusetts, Amherst, MA, USA
e-mail: cihanc58@gmail.com

B. Kane
Department of Environmental Conservation, University of Massachusetts, Amherst, MA, USA
e-mail: bkane@eco.umass.edu

Published online: 06 March 2013

wood properties on the wind-induced dynamic response of trees (Sellier et al. 2006; Moore and Maguire 2008; Sellier et al. 2008; Sellier and Fourcaud 2009). Moore and Maguire (2004) reviewed the literature pertaining to dynamics of forest-grown conifers and presented an empirical relationship, consistent with dynamic beam theory (Niklas 1992), that predicted natural frequency of such trees from the ratio of diameter at breast height (DBH) to the square of tree height. Recent work, however, has highlighted the importance of crown shape and branches on the oscillation of trees (Sellier and Fourcaud 2005; James et al. 2006; Spatz et al. 2007; Sellier and Fourcaud 2009).

Damping is critical in trees to avoid resonance and to rapidly decrease the response when wind excitation diminishes (James et al. 2006; Sellier and Fourcaud 2009). The motion of branches relative to one another and the stem has been referred to as structural (Niklas 1992), mass (James et al. 2006), or multiple resonance (Spatz et al. 2007) damping. This is an important component of the overall damping of sways of decurrent (James et al. 2006) and excurrent (James et al. 2006; Spatz et al. 2007; Moore and Maguire 2008) trees, through which wind energy is transferred between the stem and branches of varying order.

The mechanism of structural damping is presumably more important in open-grown trees. Such trees typically develop a decurrent form so that the relative proportion of branch and stem mass is the reciprocal of that of excurrent trees, but they also tend to have much less slender trunks. Open-grown trees also do not benefit from damping associated with crown collisions (Milne 1991; Rudnicki et al. 2008), so the effect of the sway motion of branches is likely to be important to the overall dynamic response of the tree.

Empirical studies (Baker 1997; James et al. 2006; Kane and James 2011) have demonstrated the effect of crown form on natural frequency of open-grown trees. In contrast to Moore and Maguire's (2004) empirical relationship to predict natural frequency, Baker (1997) showed that the natural frequency of open-grown, deciduous trees was inversely proportional to DBH. Although Baker's (1997) empirical equation predicted the mean natural frequency of Bradford Pear (*Pyrus calleryana*), predicting natural frequency of individual trees from the ratio of DBH to the square of tree height proved problematic (Kane and James 2011). Recent FE models considering mature trees have focused on plantation-grown conifers (Moore and Maguire 2008; Sellier et al. 2008). And while Rodriguez et al. (2008) examined the effect of branches on a small walnut tree (*Juglans regia* L.), it is not clear that their results can be scaled to a large tree of decurrent form. The failure of such trees presents substantial risk of damage or personal injury in developed landscapes.

Previous FE models have assumed a constant value of the elastic modulus (MOE) for the entire tree (Sellier et al. 2006), separate but constant MOE values for the stem and branches (Moore and Maguire 2008; Rodriguez et al. 2008; Sellier and Fourcaud 2009) or axial variation in MOE of the stem but constant MOE for branches (Sellier et al. 2008). Moore and Maguire (2008) noted that greater attention should be paid to axial variation in MOE of branches, which has been shown to vary in Norway maple (*Acer platanoides* L.) (Dahle and Grabosky 2010). Previous FE studies have mostly applied single frequency excitation to the tree models (Sellier and Fourcaud 2009).

A better understanding of the effect of branches on the dynamic response of large, open-grown trees will help assess and reduce the risk of failure of such trees, which can damage property and injure people. In the United States, from 1995 to 2007, 407 people died as a result of wind-related tree failures (Schmidlin 2009), and litigation often accompanies property damage and personal injury (Mortimer and Kane 2004). Given the complex crown architecture of many open-grown trees and the sparse empirical data relevant to developing mechanistic models for such trees, an initial approach to address this challenge is to use FE analysis to investigate the dynamic response of a mature, decurrent tree. In light of the identified gaps in knowledge in the dynamic response of trees under wind excitation, the objectives of this study were to investigate the effects of (a) geometric and material properties of branches, (b) crown architecture, and (c) the stem on the dynamic amplification factor at a range of wind excitation frequencies.

Materials and methods

Please see Appendix A for a list of all symbols associated with formulas throughout the text.

Base tree

All parametric models described in this section were created with reference to a base model (denoted M100) of a sugar maple (*Acer saccharum*) growing in Belchertown, MA, USA (72.413°W longitude and 42.277° N latitude). The site was formerly an institutional property with streets and buildings, and the size and crown architecture of trees (Fig. 1) were typical of those growing in residential settings in the northeastern United States. In particular, the seventh branch (Table 1) effectively served as a co-dominant stem. The diameter of the main stem is 53 cm measured 1.4 m above the ground (diameter at breast height, DBH) and the tree height is 17.1 m. Its crown is 13.7 m in height and 12.1 m in width; the ratio of minimum to

Fig. 1 Maple tree in Belchertown, MA which is used for the base model, M100

maximum crown width, measured orthogonally, is 0.74. The height, diameter, attachment angle, and azimuth of all eleven primary branches were also measured (Table 1). Branch length was not measured due to time constraints. To create the parametric tree models, selected physical properties of M100 (stem diameter; damping ratio; and the number, slenderness ratio, attachment height, attachment angle, and azimuth of branches) were changed independently. Each parametric model is fully described below.

In August 2006, strain meters that measured axial trunk displacements accurate to 0.001 mm were attached orthogonally to the stem (north or south and east or west sides) of M100 approximately 1.4 m above the ground as described by James and Kane (2008). A skidder with a cable winch (John Deere model 440D) was used to apply a point load at approximately 40 % of tree height, where the diameter of the trunk was large enough to sustain the applied load without failing. The tree was pulled and released three times, incident with each strain meter (six tests total); loads were always applied to place the strain meters in tension. Axial displacements during free sways were recorded on both strain meters (incident and orthogonal) and plotted with respect to time. The time (T) and amplitude (y) of five successive maximum displacements ($i = 1, 2, 3, 4, 5$) were used to determine damping ratio (ζ), which was calculated using the logarithmic decrement method:

$$\frac{y_i}{y_{i+1}} = \exp\frac{2\pi\zeta}{\sqrt{1-\zeta^2}}. \quad (1)$$

For each time history of displacement, a Power Spectral Density (PSD) was plotted in MATLAB (7.10.0 R2010a, Mathworks, Natick MA) and used to calculate the tree's natural frequency.

Finite element modeling

The finite element (FE) modeling program ADINA-8.5 (ADINA Software, Watertown, MA, USA) was used to conduct the analyses of all tree models. The stem and branches of M100 and all of its parametric iterations were divided into longitudinal elements of constant geometry and MOE. For each branch or stem element, MOE and diameter were separately defined before meshing the elements. The concept of local averages of random fields introduced by Bucher (2009) was used to define the properties of each element. In this method, each element is assigned properties of a homogenous material instead of using heterogeneous material properties, but the overall material variations are captured by dividing the tree model into sufficient elements.

Elements within each tree stem and branches (M100 and its parametric iterations) were modeled using Euler–Bernoulli beam elements of varying cross-sectional dimensions to model the branch taper. Branches were divided into 12 cylindrical elements of equal length. Diameter of the proximal element was from the measured value and each subsequently distal element was reduced in diameter according to the assumed slenderness value as long as the diameter of the most distal element was $\geq$2 cm. Stems were divided into elements as follows: nodes were established on the stem at the height of each branch; if the distance between two successive nodes exceeded 0.5 m, additional nodes were added at equal lengths midway between them so that no nodes were more than 0.5 m apart. The MOE of the proximal stem element was set to 10.7 GPa (Kretschmann 2010). For each subsequent element, MOE was adjusted in accordance with the slope of an empirical relationship for branches of Norway maple (Dahle and Grabosky 2010). For the elements in the distal 4.3 m of the stem (the top branch), MOE was held constant at the value of the first element in the top branch. Spatz et al. (2007) noted a decrease in MOE of branches with branch height, so MOE of the proximal element of each branch was initially assigned the MOE of the stem element to which the branch was attached. MOE can also vary with branch diameter (Niklas 1997), so MOE of each proximal branch element was adjusted approximately according to the empirical relationship developed by Spatz et al. (2007). Using their exact relationship produced unrealistically high

Table 1 Diameter, estimated mass, mass-weighted mean MOE, attachment height, azimuth, attachment angle, and the first modal frequencies of the stem and each branch of M100

M100	Diameter (m)	Mass (kg)	MOE (GPa)	Attachment height (m)	Azimuth angle (°)	Attachment angle (°)	Natural frequency (Hz)	1st Mode frequency (Hz)
Stem	0.53	1235	9.00	n/a	n/a	n/a	2.368	2.332
Top branch	0.13	69	4.60	12.80	0	0	1.070	1.641
1st Branch	0.28	393	5.08	3.23	83	44	0.693	0.756
2nd Branch	0.27	320	5.03	3.96	230	23	0.726	0.811
3rd Branch	0.27	338	4.95	5.33	68	27	0.704	0.786
4th Branch	0.08	8	4.29	5.36	180	37	1.291	1.752
5th Branch	0.11	21	4.50	5.94	22	13	1.150	1.471
6th Branch	0.06	4	3.97	6.10	354	62	1.341	2.049
7th Branch	0.32	563	5.08	6.19	298	80	0.594	0.652
8th Branch	0.19	118	4.83	7.38	157	88	0.847	0.983
9th Branch	0.17	81	4.74	7.62	47	85	0.906	1.106
10th Branch	0.12	30	4.52	8.60	109	47	1.062	1.395
11th Branch	0.06	5	4.03	9.66	111	90	1.308	2.003

The first modal frequencies were calculated using Eq. (6) (Mabie and Rogers 1972). The estimated first mode frequencies by using Eq. (6) are comparable with the results of the FE modeling

values of MOE, presumably because of different species and the disparity in branch diameter between branches used to derive the relationship and those of M100. Adjusting MOE as described produced similar mass-weighted mean values of MOE for branches of similar diameter (Table 1), with one exception: the unadjusted, mass-weighted mean MOE of the seventh branch was substantially less than branches of similar diameter (e.g., the first, second, and third branches). MOE of the proximal element of the seventh branch was increased so that the mass-weighted mean MOE of the entire branch was within the 95 % CI of the best-fit line predicting mass-weighted MOE of each branch from its diameter. MOE of subsequent elements in each branch was adjusted in accordance with the slope of an empirical relationship for branches of Norway maple (Dahle and Grabosky 2010).

The stem was assumed to be fixed at the base, and connections between branches and the stem were assumed to transfer moment and shear force at the attachments. The mass of the stem and branches was estimated assuming mean density of specimens of green wood (560 kg/m^3) from the Wood Handbook (Kretschmann 2010) and calculated volume of the stem or branch. This method will slightly overestimate branch mass because diameters were measured outside the bark, which is not as dense as the wood itself. The FE models only included the stem and primary branches. The mass of secondary and tertiary branches was included in the mass of their parent primary branch by increasing its density proportionately assuming a fractal structure between primary and higher order branches. The ratio of stem volume to the total volume of primary branches was calculated for M100. Assuming that M100 followed a fractal structure as described by Rodriguez et al. (2008), the ratio was applied to each primary branch to estimate the additional mass contributed by secondary and tertiary branches. Previous work has demonstrated that modeling branches as lumped masses attached to the stem can lead to errors of modeled natural frequencies of trees (Sellier et al. 2006; Moore and Maguire 2008), so the weight of each branch was modeled as uniformly distributed along each branch. This procedure ensured that the entire mass of the tree was included in the analysis.

The measured value of ζ from free sway tests was 18 %. This value was rounded down to 15 % to facilitate visual presentation of the parametric analyses and it did not meaningfully affect the results (as described in the "Results" section). In order to emphasize damping for the first two modes of oscillation, the Rayleigh damping coefficient (β) was assumed to be 0.001; previous studies (Sellier et al. 2006; Castro-García et al. 2008) have used similar values. If β is known, α can be calculated from Eq. (2):

$$\alpha + \beta\omega_k^2 = 2\omega_k\zeta_k \tag{2}$$

where ω_k is known from the undamped dynamic analyses and ζ is 15 %.

To validate the FE model, modal frequencies of the whole tree, the branchless stem, and each branch were determined several other ways. Natural frequency of the whole tree was determined from field tests (described above) and by using two empirical relationships. Baker (1997) developed Eq. (3) for in-leaf *Tilia* x *europaea*:

$$f_n = [0.569 - 0.0021(DBH)] \pm 0.0043[1 + 0.0026(DBH - 58.4)^2]^{1/2}. \quad (3)$$

where DBH is measured in cm and the right-hand term is the 99 % confidence interval. Substituting 53 cm into Eq. (3) yields 0.50 Hz. Mayhead (1973) developed Eq. (4) for conifers:

$$f_n = \left[0.86 + 0.74\left(\frac{H\sqrt{MH}}{DBH^2}\right)\right]^{-1} \quad (4)$$

where DBH is given in cm, H is total tree height (m) and M is tree mass (kg). Entering values of M100 into Eq. (4) gives:

$$f_n = \left[086 + 074\left(\frac{17.1\sqrt{3185(171)}}{53^2}\right)\right]^{-1} \approx 0.52\,\text{Hz} \quad (5)$$

The first four modal frequencies of the branchless stem and each branch were determined in the FE analysis (first frequency), or using Mabie and Rogers' (1972) equation for double-tapered cantilever beams (second, third, and fourth frequencies):

$$f_n = \frac{(lk)^2}{2\pi(l^2/h_1)}\sqrt{\frac{Eg}{12\rho}} \quad (6)$$

where $(lk)^2$ is a constant associated with a particular beam taper, l is the length of the element, h_1 is the thickness at the distal point of the element parallel to the direction of the applied load, E is the elastic modulus, g is gravitational acceleration, and ρ is the density of the element. Imperial units were used for these parameters to be consistent with Mabie and Rogers (1972).

Numerical method employed in dynamic analyses

The time history method used to conduct the dynamic analyses is unconditionally stable if the ratio of time step to natural period of the model ($\Delta t/T_n$) is less than or equal to 0.551 (Chopra 2007). To avoid any stability problems, particularly for higher modes, a sufficiently small time step of 0.05 s was selected for the analyses. To verify the accuracy of the prototype model, the undamped natural frequency was calculated in the FE program as 0.59 Hz (so $T_n = 1.69$). Thus, the ratio of the time-step increment to the natural period of the model is $\Delta t/T_n = 0.05/1.69 = 0.029 < 0.551$.

Material nonlinearity was ignored in the FE model because the tree response did not exceed the yield stress, so displacements and stresses remain within the elastic region. Geometric nonlinearity was neglected, because stiffness reduction caused by P-Delta effects is negligible given the relatively small mass of the stem near the top of the tree. Although the lateral deflection of M100 may be large near the top, the weight of the top branch and stem elements immediately proximal to it was much less massive than stem elements proximal to the ground, which experience very small lateral deflection. Including the P-Delta effect increased Rd on average by 1 % for the range of modeled wind frequencies.

Assumed wind loading

Since wind speed varies with height (z) above the ground (Hsu et al. 1994; Zhu et al. 2000), for each element of the tree in the FE model, wind profile (u) was determined by Eq. (7) (Panofsky and Dutton 1984), which is commonly used in engineering texts for land based and for the neutral stability of the atmosphere:

$$u = u_h(z/h)^{1/7} \quad (7)$$

where u_h is the referenced wind speed at height ($h = 1.4$ m). Wind speed profiles used in forest stands were deemed inappropriate because of the substantial reduction in wind speed below the top of the canopy. Maximum wind speed modeled was 10 m/s. The aerodynamic drag (D) applied as a harmonic function on each tree element was calculated as:

$$D = 0.5\rho_{air}u^2AC_D \quad (8)$$

where ρ is air density (assumed to be 1.226 kg/m^3), A is the frontal area of each cylindrical element of a branch or the stem, and C_D is the drag coefficient, which was assumed to vary with wind speed in accordance with Kane and Smiley's (2006) empirical relationship for small red maples (*Acer rubrum*). The distribution of drag on the tree and individual branches is shown in Fig. 2. Each model was run 38 times for wind excitation frequencies ranging between 0 and 5 Hz. Wind frequencies were incremented by 0.05 Hz for frequencies up to 1.20, 0.1 Hz for frequencies between 1.20, 2.00, and 0.50 Hz for frequencies >2.00 Hz. Multiple frequencies were investigated because of the highly variable air flow and turbulence associated with wind in developed settings (Kastner-Klein et al. 2004). Smaller increments were used at lower frequencies to better capture the low frequency response of the trees, where greater wind energy can be transferred to the tree (Baker 1995). Plots of Rd versus wind frequency in the " Results" section include interpolated values between modeled wind frequencies.

Dynamic amplification factor (Rd)

To capture the characteristics of dynamic response using a single parameter, the dynamic displacement amplification (or deformation response) factor (Rd) was selected as the

primary output of the FE models. Rd is the ratio of the maximum displacement computed from the dynamic response of a structure to the maximum displacement computed from the static response of the structure. This approach is particularly useful to evaluate systems responding in the linear range, as assumed for all tree models in this study. Rd represents a unitless function that depends on characteristics of the structure (the mass, damping, and stiffness of the tree in this case) and the forcing function (frequency in the case of a harmonic load). For a single degree of freedom (SDOF) system subject to harmonic loading, Rd can be calculated as (Chopra 2007):

$$Rd = \frac{u_0}{(u_{st})_0} = \frac{u_0}{P_0/k} = \frac{1}{[1-(\omega/\omega_n)^2]^2 + [2\zeta(\omega/\omega_n)]^2} \quad (9)$$

where ω is the frequency of the excitation function, ω_n is the natural circular frequency of the system, ζ is the damping ratio, k is the stiffness of the system, and P_0 is the amplitude of the excitation force.

For SDOF systems, Rd is plotted as a function of the frequency ratio (ω/ω_n) (Chopra 2007). There are often multiple peaks for MDOF systems, however, so Rd was plotted as a function of ω for this study, as in Fig. 3. Modal frequencies of M100 were identified where peaks in plots of the damped and undamped Rd for Node-10 (located on the stem 1.4 m above the ground) occurred at the same excitation frequency. Modal frequencies of each branch of M100 were identified where peaks in the plot of the undamped Rd for a node near the base of the branch exceeded the Rd plotted for Node-10. Figure 3 includes these plots for Node-27, near the base of the first branch, which is closest to the ground.

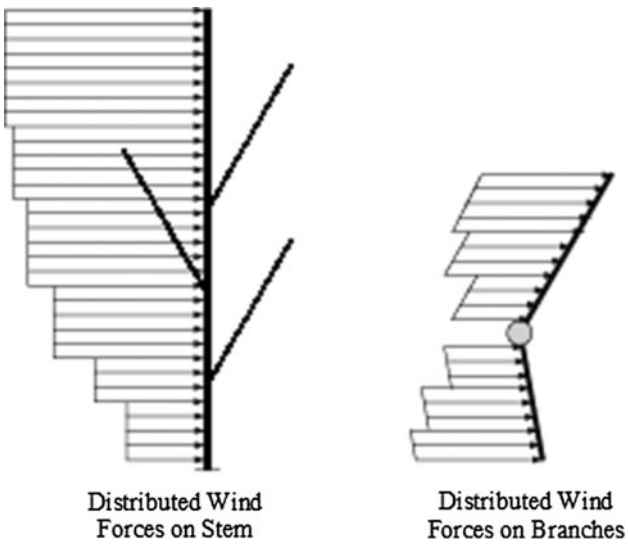

Fig. 2 Illustration of distributed wind forces on stem and branches of trees. The figure on the *left* is an elevation view, and the one on the *right* is a plan view

In civil engineering (or earthquake engineering), Eq. (10) is a common formula to calculate the total static shear force at the basement of buildings (Chopra 2007):

$$V_{bn}^{st} = \sum_{j=1}^{\infty}\sum_{n=1}^{\infty}(s_{jn}) = \sum_{j=1}^{\infty}\sum_{n=1}^{\infty}(\Gamma_{jn} m_j \Phi_{jn}) \quad (10)$$

where Γ_n is the modal participation factor of the nth mode, m_j is the mass of the jth lumped mass and ϕ_{jn} is the nth-mode shape at the location of the jth lumped mass. The modal participation factor (Γ_n) includes the modal mass (M_n) of the total system in its denominator. Thus, the ratio of m_j in Eq. (10) to the modal mass (M_n) is called mass participation of a branch or branches. To investigate the effect of branch mass on the dynamic behavior of the stem, it can be assumed that each branch mass is a lumped mass (m_j) on the stem. The shear force (s_{jn}) at the attachment of a branch to the stem depends on the branch mass. Therefore, the largest branches in Table 1 (7, 1, 3 and 2nd branches, in descending order of diameter), which contain a large portion of the total mass of the tree, cause great shear force where they attach to the stem, increasing displacement and Rd.

Parametric models

The parametric analysis used M100 as the base model. To investigate the effect of tree morphometry on Rd, each of eight parameters (stem diameter; damping ratio; MOE; and the number, height, attachment angle, azimuth and slenderness ratio of branches) was varied independently, holding the other parameters constant. A nomenclature was created to represent all the parametric models, in which the second digit refers to the number of the parameter being varied and the third digit refers to the variation of the parameter. For example, models M111, M112, M113, and M114 are the four variations of the first parameter; M121 and M122 are two variations of the second parameter, and so on. Parameters were varied in accordance with personal observations of the authors for open-grown sugar maples in the northeastern USA.

The effect of stem diameter was examined by multiplying the stem diameter of M100 by 1.25, 1.50, 1.75, and 2.00, which increased the stem diameter to 66, 79, 93, and 106 cm in models M111, M112, M113, and M114, respectively. Trees of smaller diameters were not modeled because it was intended to investigate large trees that posed a greater risk of damage if they failed. To maintain a realistic taper of the stem, the diameter of the top branch (the axial extension of the stem) was also increased by the same factors in these models.

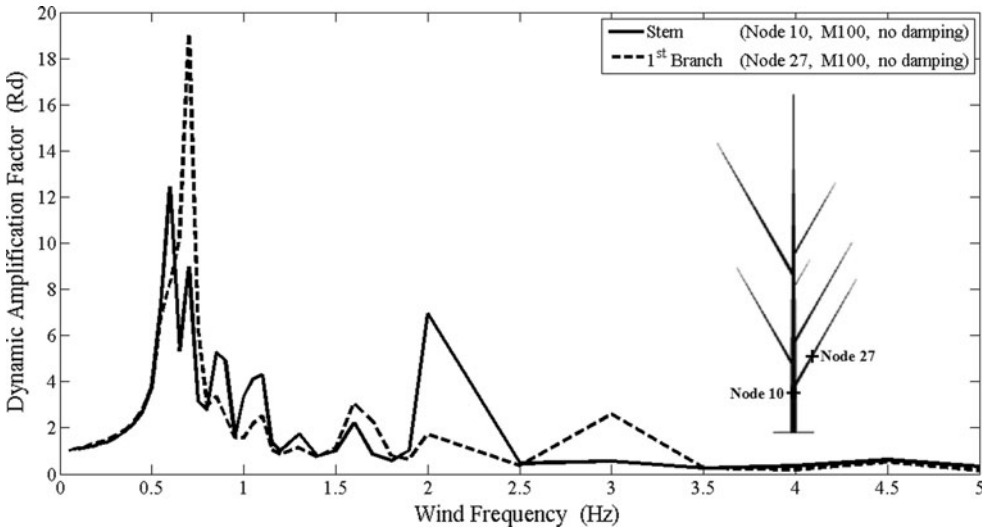

Fig. 3 Comparison of the dynamic amplification factors of the first branch and the main stem in the prototype tree. The *solid line* corresponds to Node 10, which is on the stem, 1.4 m above the ground. The *dashed line* is for Node 27, which is on the proximal element of the first branch

Branches on M100 were assumed to have a slenderness ratio of 50. This value was selected because it represented the mean slenderness (rounded to the nearest ten) of branches, the diameter of which was at least 10 % of stem diameter on a nearby sugar maple. Only larger primary branches were measured on the nearby sugar maple because it was expected, from Eq. (10), that more massive branches would exert a greater influence on Rd and that the influence of smaller primary branches was negligible. Slenderness was changed to 60 and 40 in models M121 and M122, respectively. These values represented the mean slenderness (rounded to the nearest ten) of branches the diameter of which exceeded the median and upper quartile diameters, respectively, on the nearby sugar maple. Slenderness ratio was changed by altering branch length while keeping branch diameter constant.

The number of branches on the tree was varied as follows (Fig. 4): model M130 included only the stem and the "top branch," the axial extension of the stem. Subsequent models added individual branches (see Table 1): models M131, M132, M133, and M134 added the first; first and second; first, second and third; and first, second, third and fourth branches of M100, respectively. Branches were added beginning with those closest to the ground because the first three branches had comparatively larger diameters while the fourth was of smaller diameter. This approach facilitated a comparison of the effect of branch mass and branch dynamic response on Rd. To explore the effect of spatial distribution of mass on Rd, additional models were considered. M131-7 included just the top and seventh branches. M131 was expanded by moving the first branch to different heights: 4.7 and 6.2 m. The latter height is the height of the seventh branch.

The effect of damping was examined by increasing the damping ratio from 0 to 0.20 with the following values: 0, 0.01, 0.05, 0.10, 0.15, and 0.20. The range was chosen in accordance with the maximum measured value from free sway tests on M100 and values similar to those previously reported for deciduous trees (Roodbaraky et al. 1994; Kane and James 2011). Because of the non-linear relationship between Rd and ζ (equation 13), it was expected that models with damping ratios greater than 20 % would approach the static response (few to no oscillations) so were not considered.

To assess the effect of the branch attachment heights, the attachment points were increased (M151) and decreased (M152) by 0.5 m for all branches. These models were expected to serve as a comparison to models in which branches were added, because of the consistent change in the location of mass distribution along the stem.

In addition to a model using measured branch angles (M163), models were also developed assuming constant branch angles of 40, 30 and 20° for M161, M160, and M162, respectively. These attachment angles were selected because it was observed that many branches on the sugar maple curved upwards beyond their attachment to the stem. It was not possible to measure the angle of the branch relative to its center of mass. Results demonstrated that this assumption was reasonable.

The effect of wind directionality was investigated by varying the branch azimuth angle instead of changing the direction of wind forces, which were initially assumed to be from the west. Models M171, M172, and M173 increased the azimuth of each branch by 30, 60, and 90 degrees relative to their measured azimuth.

Two models were created to investigate the effect of varying MOE axially for branches and the stem. In M181, MOE of the stem and branches was set to the constant value of 6.53 GPa, which was the mean MOE of all elements in M100, weighted by the mass of each element. In

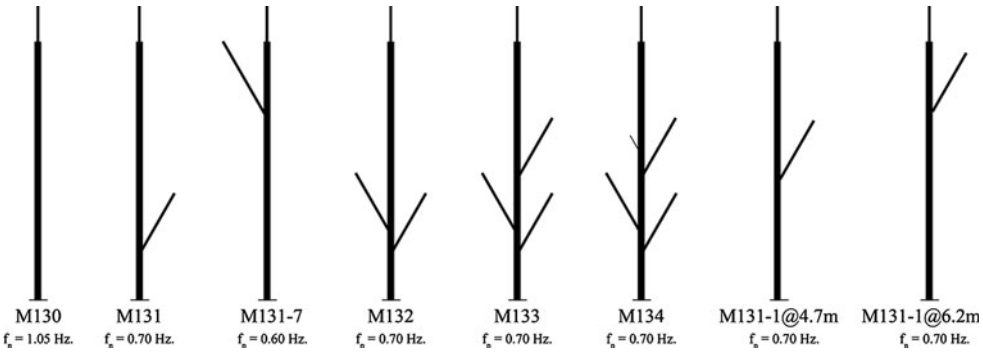

Fig. 4 Illustration of models M130, M131, M132, M133, and M134, where the parameter varied is the number of branches. M131-7 represents the tree that has only the top and seventh branch. M131-1@4.7 m and M131-1@6.2 m are for the models that attached the first branch to the trunk at 4.7 and 6.2 m above the ground, respectively

M182, MOE of each element of the stem was set to 9.0 GPa, the weighted mean of MOE of stem elements in M100; MOE of each branch element was set to 4.99 GPa, the weighted mean of MOE of all branch elements in M100.

Results

Morphometry and natural frequency of M100

Table 1 includes the estimated mass of each branch and stem and mean MOE of branches and the stem, weighted by the mass of each element in a branch or the stem. Table 1 also includes the natural frequencies of the stem and branches of M100. The mode shapes of the stem, top branch, and first branch are shown in Fig. 5. It can be seen that smaller natural frequencies correspond to branches of greater diameter because natural frequency is inversely proportional to the diameter of a beam. The circular frequency (ω_n) of a branch is the square root of the ratio of stiffness (k) and mass (m), which increase as functions of diameter raised to the fourth power and cubed, respectively:

$$\omega_n = \sqrt{k/m} \tag{11}$$

Figure 3 reveals the first three modal frequencies of the first branch (see Table 1 for values) in comparison with modal frequencies of M100. Unless stated otherwise, Rd values refer to those at Node 10 in the FE model, which is on the stem, 1.4 m above ground.

Figure 6 shows Rd of M100 as a function of wind frequency for damping ratios of 0 and 15 %. The fully damped model shows a peak at 0.59 Hz, which is greater than the value determined from pull and release tests (0.42 Hz). Although 0 % damping is unrealistic, it is included to illustrate peaks in the Rd curve that would otherwise not be visible. The peaks of the undamped plot of Rd at 0.59 and 2.0 Hz correspond to the first and the second modal frequencies of the tree; the first modal frequency is close to the first modal frequencies of the large branches and the second modal frequency is close to the first modal frequency of the stem, the second modal frequency of the medium and small sized branches and the third modal frequencies of the largest branches (Table 1). Other peaks in the undamped model correspond to modal frequencies associated with branches. The number of branches and the number of peaks in the plot are not equal because several branches have natural frequencies that are approximately equal (because they have similar diameters). For example, the first modal frequencies of the first, second, and third branches are similar (Table 1), which caused the peak in Rd near 0.7 Hz (Fig. 6).

Effects of parameters on dynamic response of tree models

Figure 7 shows Rd plotted with respect to wind frequency for M100 and models of trees with greater stem diameter. The plot can be divided into three regions, identified by ovals. The left-hand oval marks the region where the first peaks of the Rd curves occur. The first peaks reflect the first modal frequency of several large branches (Table 1). Peaks in the center oval include the natural frequency of the top branch in the models. Peaks in the right-hand oval reflect the natural frequency of the stem in each model. The frequency at which Rd was maximum increased in the center and right-hand ovals because of increased diameters of the top branch and the stem. The first modal frequencies of the stem and top branch in each model can be found in

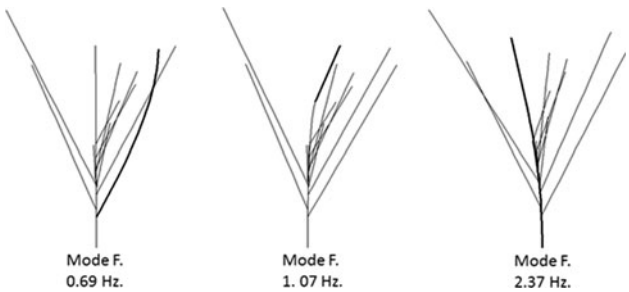

Fig. 5 Natural frequencies and mode shapes of selected members (1st branch, top branch, and main stem, respectively, from *left* to *right*)

Table 2. Peaks in Fig. 7 that coincide with natural frequencies of different branches (left-hand and center ovals) and the stem (right-hand ovals) are consistent with the mass participation of different elements in the structure (Chopra 2007). As the diameter of the stem and top branch increased, their mass participation increased, which explained why Rd of models of greater stem diameter decreased in the left-hand oval, but increased in the center and right-hand ovals.

Changes in slenderness ratio were introduced in the models by changing the length (and, consequently, the mass) of branches, which altered natural frequency of the branches as expected from the dynamics of a cantilever beam with uniformly distributed mass and elasticity (Chopra 2007):

$$f_n \propto \sqrt{\dot{E}I/\dot{m}L^4} \tag{12}$$

where $\dot{E}$ is the distributed elastic modulus, I is the moment of inertia, and $\dot{m}$ and L are the distributed mass and length, respectively, of the beam. As slenderness decreased, Rd increased (Fig. 8) because the natural frequency of larger branches became closer to the natural frequency of the stem and top branch (Table 1), which had slenderness ratios of 24 and 33, respectively. Changing the assumed value of slenderness from 50 to 60, caused a peak at 0.40 Hz (Fig. 8), consistent with the value determined from free sway tests.

The effect of adding branches on Rd again captured the effect of mass participation (Chopra 2007) of different elements in the system. The addition of branches of similar natural frequencies increased the magnitude of Rd at the resonance frequency associated with the branches and decreased the magnitude of Rd at resonance frequencies associated with the stem and top branch (Fig. 9). Rd of M130 (just the stem and top branch) had maxima at 1.07 and 2.50 Hz, which corresponded to the natural frequencies of the top branch and stem, respectively (Table 1). Adding the first branch (M131) added another peak of Rd at 0.65 Hz, close to the natural frequency of the first branch (Table 1). Adding the first branch also reduced the magnitude of Rd at 1.07 and 2.50 Hz because the natural frequency of the first branch was not similar to that of either the stem or top branch. This pattern recurred when the second (M132) and third (M133) branches were added. Adding the fourth branch did not meaningfully alter Rd because of the small diameter (and thus small mass) of the fourth branch (Table 1). Adding the seventh branch to M130 (M131-7) shifted the left-hand peak of Rd to coincide with the natural frequency of the seventh branch. It is not coincidental that the natural frequency of the seventh branch was similar to the natural frequency of M100 because the seventh branch is the most massive and it is also located higher on the stem than other large branches (Table 1). Increasing the height of the first branch (M131-1) resulted in similar reductions of the magnitude of Rd at the resonance frequencies associated with the top branch (1.07 Hz) and stem (2.50 Hz), as well as increasing the magnitude of Rd near the resonance frequency of the first branch (0.69 Hz) (Fig. 10). As the height at which the shear force and moment of the first branch were transferred to the trunk increased, the magnitude of Rd (a) increased at the resonance frequency of the first branch (the first peaks region in Fig. 10), but (b) decreased at the resonance frequencies corresponding to the top branch and stem (second and third peaks regions, respectively, in Fig. 10).

Figure 11 illustrates the non-linear decrease in the magnitude of Rd with increasing damping as expected from Eq. (9). For damping ratios less than 10 %, modal frequencies associated with different branches and the stem

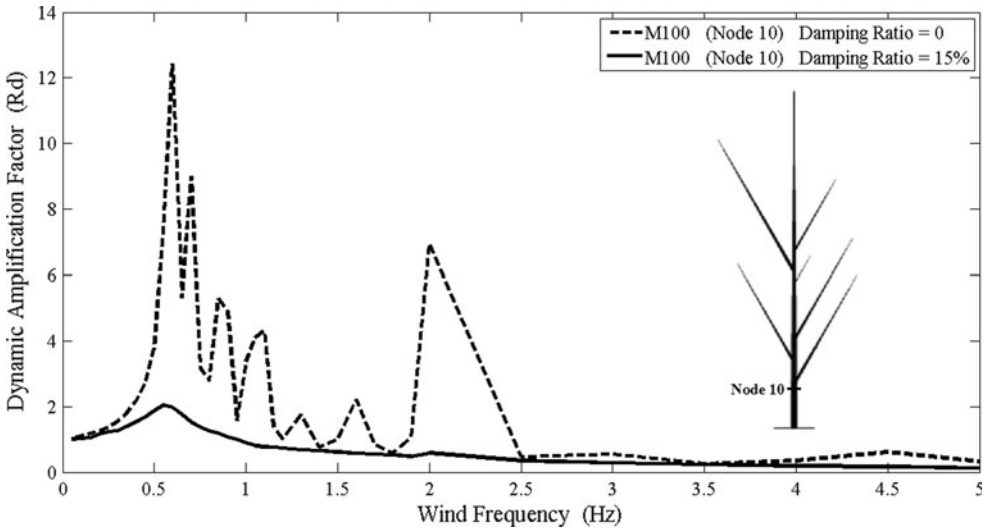

Fig. 6 Dynamic amplification factor (Rd) plotted against wind frequency for the undamped and damped (15 %) MDOF systems of the prototype tree (M100) subjected to harmonic wind forces. Values of Rd are from Node 10 which is on the stem, 1.4 m above ground

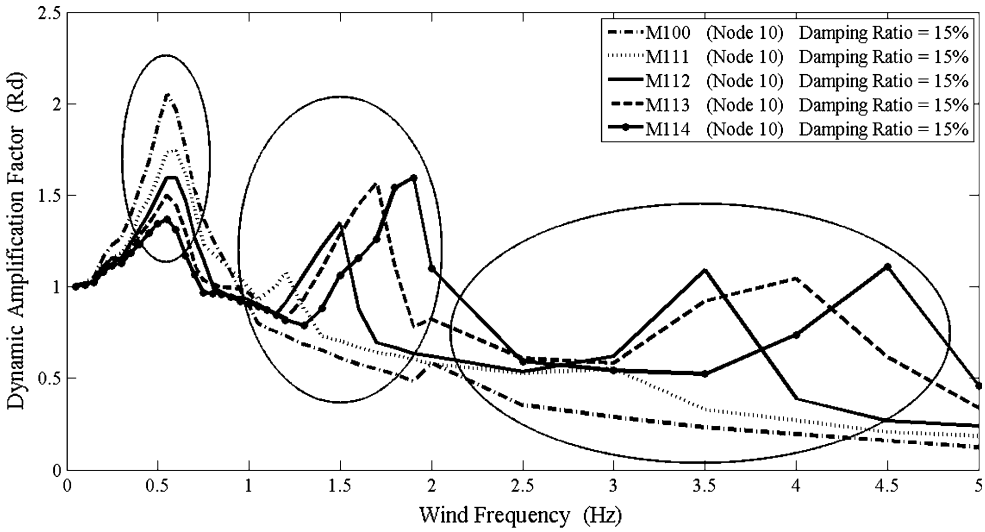

Fig. 7 Dynamic amplification factor (Rd) in terms of wind frequency for the selected models (M100, M111, M112, M113, M114). Values of Rd are from Node 10 which is on the stem, 1.4 m above ground

Table 2 Diameter and estimated first modal frequency of the stem and top branch in models shown in Fig. 11

Model	Stem		Top branch	
	Diameter (m)	Frequency (Hz)	Diameter (m)	Frequency (Hz)
M100	0.53	2.50	0.13	1.05
M111	0.66	3.00	0.16	1.20
M112	0.79	3.50	0.20	1.45
M113	0.93	4.00	0.23	1.70
M114	1.06	4.50	0.26	1.85

are obvious. These modal frequencies disappear, however, as damping increases beyond the measured value from free sway tests, and the plot of Rd for ζ of 15 and 20 % is nearly identical. The small values of Rd for $\zeta = 15$ and 20 % illustrate the heavy damping observed in the free sway tests.

Altering the height, attachment angle and azimuth of branches did not have a measurable effect on Rd (data not presented). Although changing the attachment angle of branches altered the spatial distribution of branches mass, the shear force and moment of the swaying branch were still transferred at the same height on the stem. The small magnitude and global application of change may have also limited the effect on Rd. The negligible effect of altering branch azimuth on Rd was consistent with the natural frequency of the tree measured during pull and release tests. Empirically determined values of natural frequency were similar for initial displacement in the north–south (0.40) and east–west (0.42) directions.

Assuming a constant MOE for the entire tree (M181) substantially increased Rd (Fig. 12). This was expected because the fundamental frequency of each element in the model would be more similar because each element had the same value of MOE [according to Eq. (12)]. The increase

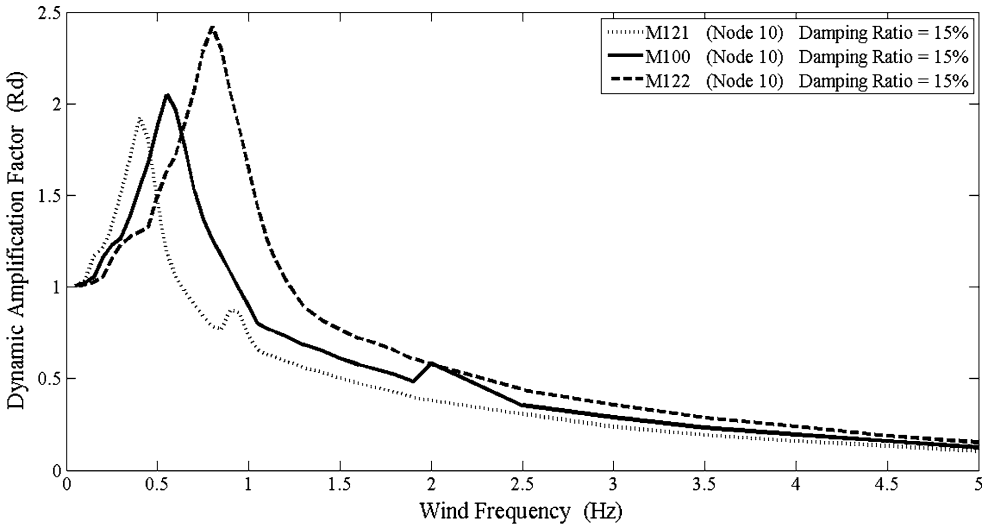

Fig. 8 Dynamic amplification (Rd) factor in terms of wind frequency for the selected models, M100, M121, and M122. Values of Rd are from Node 10 which is on the stem, 1.4 m above ground

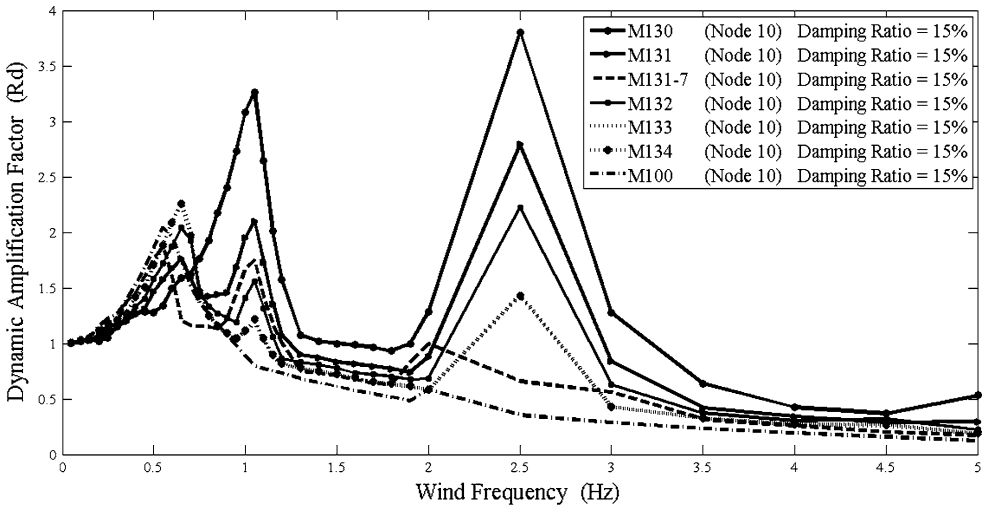

Fig. 9 Dynamic amplification factor (Rd) in terms of wind frequency for the models (M100, M130, M131, M131-7, M132, M133, and M134). Values of Rd are from Node 10 which is on the stem, 1.4 m above ground

in the frequency at which the maximum Rd of M181 occurred was also expected because MOE of the seventh branch (at which natural frequency the peak Rd occurred in M100) increased, so its natural frequency was expected to increase according to Eq. (12). Assuming different, but constant values of MOE for stem and branches (M182) slightly reduced Rd relative to M100. This result was also expected because there was a greater disparity between natural frequency of the seventh branch and that of the stem and top branch. The resonance frequency was slightly less for M182 because the natural frequency of the seventh branch would be slightly less assuming the slightly smaller value of MOE for that branch [by Eq. (12)].

Discussion

This study was the first attempt to construct a FE model of a large, open-grown tree of decurrent form. Previous FE models have focused on smaller trees (Sellier et al. 2006; Rodriguez et al. 2008) or plantation-grown conifers (Moore and Maguire 2008; Sellier et al. 2008). The estimated mass of M100 (3,185 kg) and the ratio of branch mass to stem mass (1.4) were significantly larger than Douglas-firs (Moore and Maguire 2008). Slenderness of the stem of M100 either including (32) or excluding (24) the top branch was also smaller than previous studies considering dynamic behavior of trees (Moore and Maguire 2005; Sellier and Fourcaud 2005; Jönsson et al. 2007; Spatz et al. 2007; Rodriguez et al. 2008; Sellier and Fourcaud 2009).

This study also incorporated axial variation of MOE for the stem and branches, but the base value of MOE was taken from the literature (Kretschmann 2010), rather than measured directly. The latter approach yields an "equivalent MOE" that has produced mixed results (Sellier et al. 2006; Moore and Maguire 2008). An average value from the literature was chosen because earlier tests of sugar maples at the site (Kane unpublished data) revealed a wide range of values of MOE among trees. In light of Sellier et al. (2006) caution regarding inter-tree variability with respect to MOE, and since it was not possible to measure equivalent MOE for the modeled sugar maple, an average value from the literature was chosen. It is not clear whether using a constant equivalent MOE would have similarly altered the plot of Rd as M181 did. The example of M181 demonstrates the importance of considering variation in MOE in future work, and is consistent with studies that have shown that sway characteristics are influenced by MOE of the stem (Sellier and Fourcaud 2009) and branches (Moore and Maguire 2008). In contrast, Sellier et al. (2006) assumption of a constant equivalent MOE for the entire tree was justified by close agreement of measured and modeled natural frequency of a small maritime pine (*Pinus pinaster* Ait.). This inconsistency with the example of M181 may have been due to the difference in tree size and relative proportion of crown and stem mass of the sugar maple.

The effect of crown architecture on natural frequency has been illustrated previously (James et al. 2006; Spatz et al. 2007; Sellier and Fourcaud 2009) and previous work has shown a similar difference between natural frequency of the stem compared to the whole tree (Moore and Maguire 2005; Sellier and Fourcaud 2005; Spatz et al. 2007). Results of the current study demonstrate the significant effect of large branches on sway response, consistent with mass participation (Chopra 2007) of different elements of the structure. Previous authors have speculated that the effect of large branches in a tree crown made it more difficult to explain empirical data with simplified theoretical approaches (Baker 1997; Kane and James 2011). The effect of large branches was also contingent upon their location in the crown. Altering the height of the

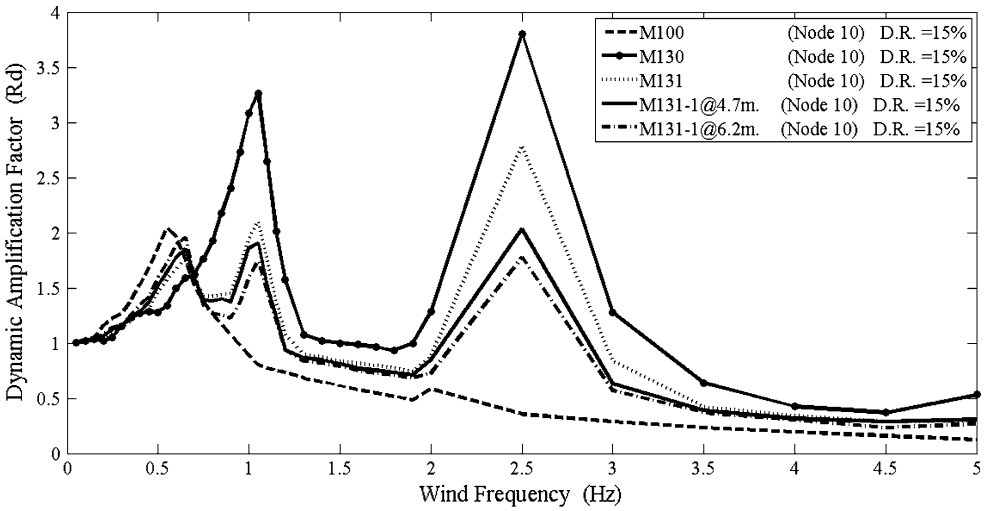

Fig. 10 Dynamic amplification factor (Rd) in terms of wind frequency for the models (M100, M130, and M131-1). The latter model was constructed to locate the mass of the first branch at its actual height (3.2 m), as well as 4.7 and 6.2 m (which is the height of the seventh branch). Values of Rd are from Node 10 which is on the stem, 1.4 m above ground

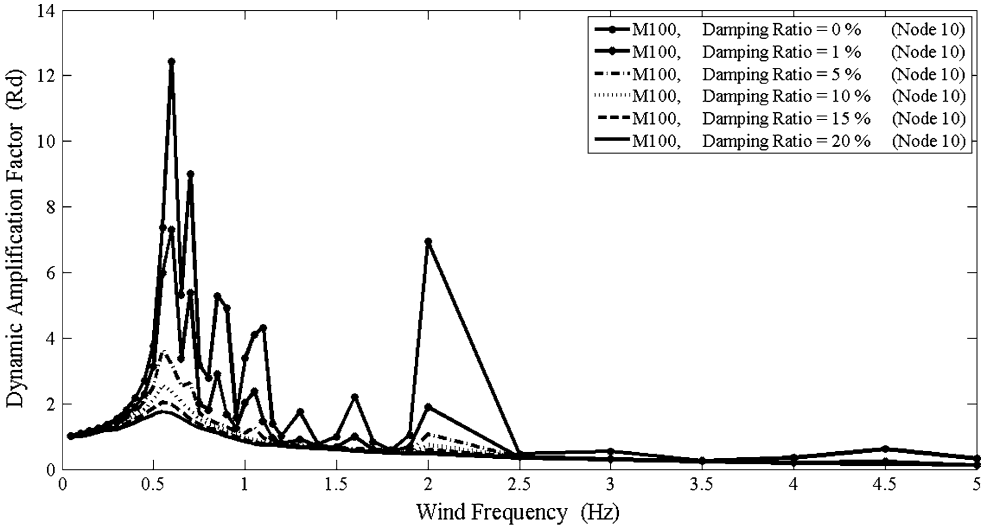

Fig. 11 Dynamic amplification factor (Rd) in terms of wind frequency for the base model (M100) with varying amounts of damping ranging from 0 to 20 % of critical. Values of Rd are from Node 10, which is on the stem, 1.4 m above ground

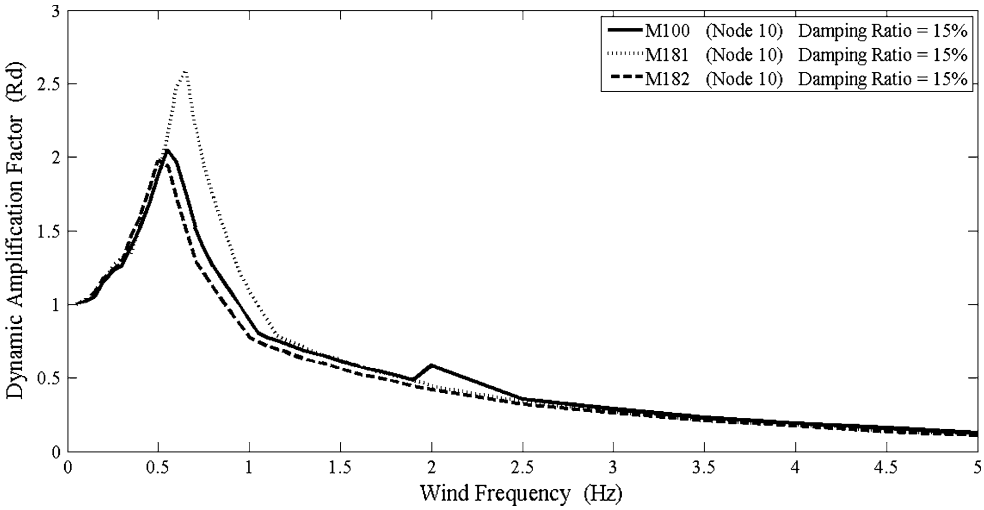

Fig. 12 Dynamic amplification factor (Rd) in terms of wind frequency for models M181, M100 and M182. Values of Rd are from Node 10, which is on the stem, 1.4 m above ground

first branch changed the magnitude of Rd in a predictable way. A large branch has a greater effect on the tree when it is located higher in the crown because the shear force and moment associated with the sway of the branch are transferred to a less massive segment of the stem. This observation, as well as the absence of maxima of Rd associated

with the natural frequencies of the top branch and stem in M100, provides additional evidence of mass participation, and is consistent with James et al. (2006) observations of mass damping. Examining Rd through a wide range of wind frequencies facilitated the illustration of mass participation, as shown by the reduced magnitude of Rd at resonance frequencies associated with the stem and top branch. The lack of effect on Rd due to changing the height of branches was not consistent with the effect of increasing the height at which the first branch was attached. This disparity was due to (a) a comparatively smaller magnitude of change to the height of branches and (b) the global application of these changes, rather than changing a single branch.

The modeled natural frequency of M100 fits within the 99 % confidence interval of Eq. (3) (Baker 1997), but it was 19 % less than the values calculated in Eq. (5) (Mayhead 1973). This disparity was not surprising because Eq. (5) was developed from trees of excurrent form.

Although it was convenient that adjusting the assumed value of slenderness resulted in a modeled natural frequency of M100 much closer to the empirical value measured in free sway tests, the result may simply be serendipitous. Results of the parametric analysis of slenderness must therefore be interpreted cautiously. The important effect of slenderness on both the magnitude of Rd and the resonance frequency underscores the need for additional work to measure the slenderness of branches and model its effect on sway motion. Concomitant with slenderness of branches, future work should more carefully account for the curvature of branches on open-grown trees to better define the spatial distribution of branch mass.

The effect of large branches on both the magnitude of Rd and the resonance frequency is clearly important in decurrent trees. Pruning to remove lower branches in the crown of excurrent trees did not substantially alter natural frequency and damping until most of the branches had been removed (Mayhead et al. 1975; Moore and Maguire 2005). Removing the seventh branch of M100, in contrast, would have removed 18 and 29 % of the total tree mass and crown mass, respectively. For decurrent amenity trees, predicting the natural frequency of large branches in the crown has important implications for pruning that warrant additional investigation. For example, removing one large branch from a crown that includes several branches of similar diameter may reduce Rd more effectively than pruning an equivalent amount of mass from several smaller branches. This approach ignores possible physiological and esthetic constraints on pruning, but a better understanding of the mechanical effects of pruning may lead to alternative approaches to pruning that more effectively reduce the risk of branch or tree failure.

The parametric analysis of Rd is useful to illustrate one aspect of the likelihood of failure of a tree, but, additional factors must also be considered for tree risk assessment. Among these are parameters to describe the wind [e.g., turbulence spectra studied by Sellier et al. (2008)] and the effect of structural defects such as decay (Kane and Ryan 2004) and poor branch attachments (Kane and Clouston 2008), which can reduce load at which trees fail. Models needed to evaluate the risk of failure of decurrent trees may be simplified and made more efficient given a better understanding of the main parameters that affect their dynamic response. However, the importance of large branches highlights the need to carefully assess crown architecture of individual trees; and additional work on parameters such as slenderness and MOE is clearly necessary.

Acknowledgments Charlie Burnham, Mike Geryk, and Alan Snow (MA DCR); and Dan Pepin (University of Massachusetts-Amherst) helped collect data. TREE Fund's Mark S. McClure Biomechanics Fellowship.

Appendix: Acronyms and Abbreviations

Y	Displacement
f_n	Natural frequency in Hz
ζ	Damping ratio
α, β	Rayleigh damping coefficients
ω_k	Fundamental circular frequency in the Rayleigh damping equation
ζ_k	Damping ratio for the fundamental frequency in Rayleigh damping equation
H	Tree height (m)
M	Tree mass in (kg)
lk	Mode frequency factor for various taper ratios of cantilever beams
l	Length of tapered cantilever beams
h_1	Thickness (in) at the distal point of the tapered cantilever beams parallel to the direction of the applied load
E	Modulus of elasticity of tapered cantilever beams (psi)
g	Gravitational acceleration (in/s^2)
ρ	Density of tapered cantilever beams (lb/in^3)
Δt	Time step in dynamic analysis
T_n	Natural period (sec)
$u(z)$	Wind profile with respect to height, z
u_h	Referenced wind speed at height, h (1.4 m)
D	Harmonic drag force on tree elements
ρ_{air}	Air density
A	Frontal area of tree elements

C_D	Drag coefficient
Rd	Dynamic displacement amplification factor
P_0	Amplitude of excitation (wind) force
ω	Circular frequency of excitation (wind) force
ω_n	Natural circular frequency
k	Stiffness of systems (SDOF or MDOF)
m	Mass of systems (SDOF or MDOF)
$(u_{st})_0$	Maximum static displacement
u_0	Maximum dynamic displacement
I	Moment of inertia of cross-sections
$\dot{m}$	Distributed mass on a cantilever beam
$\dot{E}$	Distributed elasticity on a cantilever beam

References

Baker CJ (1995) The development of a theoretical model for the windthrow of plants. J Theor Biol 175(3):355–372. doi:10.1006/jtbi.1995.0147

Baker CJ (1997) Measurements of the natural frequencies of trees. J Exp Bot 48(5):1125–1132. doi:10.1093/jxb/48.5.1125

Blackburn P, Petty JA, Miller KF (1988) An assessment of the static and dynamic factors involved in windthrow. Forestry 61(1):29–43. doi:10.1093/forestry/61.1.29

Bucher C (2009) Computational analysis of randomness in structural mechanics vol v 3. Taylor and Francis, Leiden

Castro-García S, Blanco-Roldán G, Gil-Ribes J, Agüera-Vega J (2008) Dynamic analysis of olive trees in intensive orchards under forced vibration. Trees Struct Funct 22(6):795–802. doi:10.1007/s00468-008-0240-9

Chopra AK (2007) Dynamics of Structures: Theory and Applications to Earthquake Engineering. Pearson/Prentice Hall, New Jersey

Dahle GA, Grabosky JC (2010) Variation in modulus of elasticity (E) along Acer platanoides L. (Aceraceae) branches. Urban For Urban Green 9(3):227–233. doi:10.1016/j.ufug.2010.01.004

England AH, Baker CJ, Saunderson SET (2000) A dynamic analysis of windthrow of trees. Forestry 73(3):225–238. doi:10.1093/forestry/73.3.225

Gardiner B, Byrne K, Hale S, Kamimura K, Mitchell SJ, Peltola H, Ruel J-C (2008) A review of mechanistic modelling of wind damage risk to forests. Forestry 81(3):447–463

Hsu SA, Meindl EA, Gilhousen DB (1994) Determining the power-law wind-profile exponent under near-neutral stability conditions at sea. J Appl Meteorol Climatol 33(6):757–765. doi:10.1175/1520-0450(1994)033<0757:dtplwp>2.0.co;2

James KR, Kane B (2008) Precision digital instruments to measure dynamic wind loads on trees during storms. Agric For Meteorol 148(6–7):1055–1061. doi:10.1016/j.agrformet.2008.02.003

James KR, Haritos N, Ades PK (2006) Mechanical stability of trees under dynamic loads. Am J Bot 93(10):1522–1530. doi:10.3732/ajb.93.10.1522

Jönsson MT, Fraver S, Jonsson BG, Dynesius M, Rydgård M, Esseen P-A (2007) Eighteen years of tree mortality and structural change in an experimentally fragmented Norway spruce forest. For Ecol Manage 242(2–3):306–313. doi:10.1016/j.foreco.2007.01.048

Kane B, Clouston PL (2008) Tree pulling tests of large shade trees in the genus acer. Arboric Urban For 34(2):101–109

Kane B, James KR (2011) Dynamic properties of open-grown deciduous trees. Can J For Res 41(2):321–330. doi:10.1139/x10-211

Kane BCP, Ryan HDP (2004) The accuracy of formulas used to assess strength loss due to decay in trees. J Arboric 30(6):347–356

Kane B, Smiley ET (2006) Drag coefficients and crown area estimation of red maple. Can J For Res 36(8):1951–1958. doi:10.1139/x06-086

Kastner-Klein P, Berkowicz R, Britter R (2004) The influence of street architecture on flow and dispersion in street canyons. Meteorol Atmos Phys 87(1):121–131. doi:10.1007/s00703-003-0065-4

Kerzenmacher T, Gardiner B (1998) A mathematical model to describe the dynamic response of a spruce tree to the wind. Trees Struct Funct 12(6):385–394. doi:10.1007/s004680050165

Kretschmann DE (2010) Mechanical Properties of Wood. Wood Handbook, Wood as an Engineering Material, vol 5. Department of Agriculture, Forest Service, Forest Products Laboratory, Madison

Mabie HH, Rogers CB (1972) Transverse vibrations of double-tapered cantilever beams. J Acoust Soc Am 51(5B):1771–1774

Mayhead GJ (1973) Swaying periods of forest trees. Scott For 27:19–23

Mayhead GJ, Gardiner JBH, Durrant DW (1975) A Report on the Physical Properties of Conifers in Relation to Plantation Stability. Forestry Commission Research and Development Division, Great Britain

Milne R (1991) Dynamics of swaying of Picea sitchensis. Tree Physiol 9(3):383–399. doi:10.1093/treephys/9.3.383

Moore JR, Maguire DA (2004) Natural sway frequencies and damping ratios of trees: concepts, review and synthesis of previous studies. Trees Struct Funct 18(2):195–203. doi:10.1007/s00468-003-0295-6

Moore JR, Maguire DA (2005) Natural sway frequencies and damping ratios of trees: influence of crown structure. Trees Struct Funct 19(4):363–373. doi:10.1007/s00468-004-0387-y

Moore JR, Maguire DA (2008) Simulating the dynamic behavior of Douglas-fir trees under applied loads by the finite element method. Tree Physiol 28(1):75–83. doi:10.1093/treephys/28.1.75

Mortimer MJ, Kane B (2004) Hazard tree liability in the United States: uncertain risks for owners and professionals. Urban For Urban Gree 2(3):159–165. doi:10.1078/1618-8667-00032

Niklas KJ (1992) Plant Biomechanics: An Engineering Approach to Plant Form and Function. University of Chicago Press, Chicago

Niklas KJ (1997) Size- and age-dependent variation in the properties of sap- and heartwood in black locust (robinia pseudoacacia L.). Ann Bot 79(5):473–478. doi:10.1006/anbo/79.5.473

Nowak DJ, Dwyer JF (2007) Understanding the Benefits and Costs of Urban Forest Ecosystems. In: Kuser JE (ed) Urban and Community Forestry in the Northeast. Springer Netherlands, pp 25–46 doi:10.1007/978-1-4020-4289-8_2

Nowak DJ, Stevens JC, Sisinni SM, Luley CJ (2002) Effects of urban tree management and species selection on atmospheric carbon dioxide. J Arboric 28(3):113–122

Oliver HR, Mayhead GJ (1974) Wind measurements in a pine forest during a destructive gale. Forestry 47(2):185–194. doi:10.1093/forestry/47.2.185

Panofsky HA, Dutton JA (1984) Atmospheric turbulence: models and methods for engineering applications. Wiley, New York

Peltola HM (2006) Mechanical stability of trees under static loads. Am J Bot 93(10):1501–1511

Rodriguez M, deLangre E, Moulia B (2008) A scaling law for the effects of architecture and allometry on tree vibration modes suggests a biological tuning to modal compartmentalization. Am J Bot 95(12):1523–1537. doi:10.3732/ajb.0800161

Roodbaraky HJ, Baker CJ, Dawson AR, Wright CJ (1994) Experimental observations of the aerodynamic characteristics of urban trees. J Wind Eng Ind Aerodyn 52:171–184. doi:10.1016/0167-6105(94)90046-9

Rudnicki M, Meyer T, Lieffers V, Silins U, Webb V (2008) The periodic motion of lodgepole pine trees as affected by collisions with neighbors. Trees Struct Funct 22(4):475–482. doi:10.1007/s00468-007-0207-2

Saunderson SET, England AH, Baker CJ (1999) A dynamic model of the behaviour of sitka spruce in high winds. J Theor Biol 200(3):249–259. doi:10.1006/jtbi.1999.0983

Schmidlin T (2009) Human fatalities from wind-related tree failures in the United States, 1995–2007. Nat Hazards 50(1):13–25. doi:10.1007/s11069-008-9314-7

Sellier D, Fourcaud T (2005) A mechanical analysis of the relationship between free oscillations of Pinus pinaster Ait. saplings and their aerial architecture. J Exp Bot 56(416):1563–1573. doi:10.1093/jxb/eri151

Sellier D, Fourcaud T (2009) Crown structure and wood properties: influence on tree sway and response to high winds. Am J Bot 96(5):885–896. doi:10.3732/ajb.0800226

Sellier D, Fourcaud T, Lac P (2006) A finite element model for investigating effects of aerial architecture on tree oscillations. Tree Physiol 26(6):799–806. doi:10.1093/treephys/26.6.799

Sellier D, Brunet Y, Fourcaud T (2008) A numerical model of tree aerodynamic response to a turbulent airflow. Forestry 81(3):279–297. doi:10.1093/forestry/cpn024

Spatz HC, Brüchert F, Pfisterer J (2007) Multiple resonance damping or how do trees escape dangerously large oscillations? Am J Bot 94(10):1603–1611. doi:10.3732/ajb.94.10.1603

Zhu J, Matsuzaki T, Sakioka K (2000) Wind speeds within a single crown of Japanese black pine (Pinus thunbergii Parl.). For Ecol Manage 135(1–3):19–31. doi:10.1016/s0378-1127(00)00295-4